

Soliton Trapping in Disordered Lattice

Zhi-Yuan Sun*, Shmuel Fishman†

Department of Physics,

Technion-Israel Institute of Technology, Haifa 32000, Israel

Avy Soffer‡

Department of Mathematics,

Rutgers University, New Jersey 08854, U.S.A

Abstract

Dynamics of solitons of the Ablowitz-Ladik model in the presence of a random potential is studied. In absence of the random potential it is an integrable model and the solitons are stable. As a result of the random potential this stability is destroyed. In some regime, for short times particle-like dynamics with constant mass is found. There is another regime, where particle-like dynamics with varying mass takes place. In particular an effective potential is found. It predicts correctly changes in the direction of motion of the soliton. This potential is a scaling function of time and strength of the potential, leading to a relation between the first time when the soliton changes direction and the strength of the random potential.

PACS number(s): 05.45.Yv, 42.65.Tg

Keywords: Ablowitz-Ladik model; random potential; soliton trapping; particle approach

*with e-mail address as sunzhiyuan137@aliyun.com

†with e-mail address as fishman@physics.technion.ac.il

‡with e-mail address as soffer@math.rutgers.edu

I. INTRODUCTION

Solitons are one of the most remarkable manifestations of nonlinearity. They are found for continuous systems for the Nonlinear Schrödinger Equation (NLSE) in one dimension (1D) [1]. On the lattice mobile solitons are found for the model introduced by Ablowitz and Ladik (AL) [2], while for the ordinary NLSE on a lattice, a mobile soliton is only an approximate concept. Both lattice and in the continuum disorder tend to affect and typically destroy solitons. In the present work this will be studied for a 1D lattice in the framework of the AL model.

For the continuous system, early numerical work of Bronski [3] indicates that, a NLSE soliton becomes trapped in the random media when its kinetic energy decreases sufficiently and is of comparable size to the background potential. Akkermans et.al. [4] numerically show that a soliton bounces back and forth between high potential barriers in the attractive Bose-Einstein condensates in the framework of the Gross-Pitaevskii Equation with strong disorder. In addition, like the Anderson localization of linear waves in random media, some authors relate the localization of solitons in disordered environment to *Anderson localization* [5, 6].

In absence of a random potential the AL model is

$$i\frac{\partial\psi_n}{\partial t} = -(\psi_{n-1} + \psi_{n+1})(1 + |\psi_n|^2) , \quad (1)$$

where ψ_n is the wavefunction on site n at time t . The integrability is manifested by the existence of a mobile soliton solution [7, 8]

$$\psi_n(t) = \frac{\sinh(\mu)}{\cosh[\mu(n-x)]} \exp[ik(n-x) + i\alpha] , \quad (2)$$

where the time-dependent parameters x and α can be expressed as

$$\dot{x} = 2\frac{\sinh(\mu)}{\mu} \sin(k) , \quad (3a)$$

$$\dot{\alpha} = 2[\cosh(\mu) \cos(k) + \frac{k}{\mu} \sinh(\mu) \sin(k)] . \quad (3b)$$

From (2) we see that $\frac{1}{\mu}$ characterizes the width of the soliton and x is its center. On the other hand, the AL equation has two conserved quantities, the first of which can be defined as the mass of the soliton solution [7–9]

$$M_s = \sum_{n=-\infty}^{\infty} \ln(1 + |\psi_n|^2) , \quad (4)$$

while the second can be defined as the momentum of the motion [7–9]

$$P = i \sum_{n=-\infty}^{\infty} (\psi_n \psi_{n+1}^* - \psi_n^* \psi_{n+1}) , \quad (5)$$

where $*$ denotes the complex conjugation. For the soliton solution (2) we can calculate that (also can see Appendix of [7])

$$M_s = 2\mu , \quad (6)$$

and

$$P = M_s \dot{x} = 4 \sinh(\mu) \sin(k) . \quad (7)$$

Therefore M_s can be indeed considered as the mass of the soliton.

In the present work we will study solitons for the AL model with a random potential defined by

$$i \frac{\partial \psi_n}{\partial t} = -(\psi_{n-1} + \psi_{n+1})(1 + |\psi_n|^2) + \varepsilon_n \psi_n , \quad (8)$$

where ε_n are independent random variables uniformly distributed in the interval $[-\frac{W}{2}, \frac{W}{2}]$. For the continuous version, two early reviews [10, 11] have addressed the propagation of solitons in disordered systems; in the works by Bronski [3, 12] and Garnier [13], they show two regimes for the NLSE soliton propagation. In one regime, the soliton mass decays while its velocity approaches a constant; in the other regime, the soliton mass approaches a constant while its velocity decays very slowly. Garnier further applied a perturbation theory of the inverse scattering transform to confirm that similar two regimes are found for the AL solitons with on-site random potential (in the limit of zero randomness) [14]. Which regime is relevant depends on the value of the initial mass of the AL soliton. For large μ , the mass approaches a constant, while for small μ , the velocity approaches a constant.

However, we will show numerically, for the weak randomness, the large soliton will be trapped before its velocity decreases to zero. Additionally, we will find a regime in which the AL soliton has possibility to be accelerated on the average by the randomness. We will also characterize the regime where soliton can be trapped by the disorder using a particle approach.

II. SOLITON PROPAGATION IN A DISORDERED LATTICE

In this section we will study the solution of Eq. (8) numerically and semianalytically in order to develop an intuitive picture of the soliton dynamics. The initial soliton is the one found for a chain without disorder, given by (2) with

$$x = 0, \quad \dot{x} > 0 , \quad (9a)$$

$$M_s(t = 0) = 2\mu . \quad (9b)$$

The numerical solution is obtained propagating the soliton by Eq. (8). To save computer resources we use a coordinate system moving with the center of mass of the soliton, consisting of N sites, centered on soliton. The computation is performed using a 4th-order Runge-Kutta type algorithm in time, and an absorbing-wave boundary condition on sites. We define the following quantities:

soliton mass

$$M_s^{(N)} = \sum_n^N \ln(1 + |\psi_n|^2) ; \quad (10)$$

center of mass coordinate

$$x^{(N)} = \sum_n^N n \ln(1 + |\psi_n|^2) / M_s^{(N)} , \quad (11)$$

and the second moment

$$m_2^{(N)} = \sum_n^N (n - x^{(N)})^2 \ln(1 + |\psi_n|^2) , \quad (12)$$

while the soliton velocity is

$$v = \Delta x^{(N)} / \Delta t , \quad (13)$$

where $\Delta x^{(N)}$ is the change of $x^{(N)}$ during the time interval Δt (here we use $\Delta t = 0.001$). In addition, two parameters, that characterize the soliton are introduced in simulation: one is the amplitude of the soliton

$$A_s = \max_n |\psi_n|^2 , \quad (14)$$

the other one is the soliton width, defined as the minimum N_w satisfying

$$\sum_{-(N_w-1)/2}^{(N_w-1)/2} \ln(1 + |\psi_n|^2) / M_s^{(N)} \geq 1 - \delta , \quad (15)$$

here $\delta = 0.01$ [note that, in simulation we first find the peak position of the soliton, then (15) is calculated with this position as the center].

There are basically 3 regimes characterized by the initial value of μ :

$$(A) \quad \mu \gg 1 ; \quad (16a)$$

$$(B) \quad \mu \approx 1 ; \quad (16b)$$

$$(C) \quad \mu \ll 1 . \quad (16c)$$

A. The regime $\mu \gg 1$

We choose an AL soliton with $\mu = 3$, which has more than 99% mass concentrating in 3 lattice sites ($N_w = 3$). The reason for picking up a soliton of such narrow width is based on the fact that it is compact enough to admit low level of mass radiation resulting of randomness. Such low-level radiation is necessary for observing possible soliton acceleration in our numerical simulation. The initial velocity of the soliton is chosen as $\dot{x}(t = 0) = 1$, and one realization of the random potential with $W = 0.1$ is used (note that $0.04 \lesssim W \lesssim 0.1$ can be seen as the weak randomness in our discussion, below this interval is considered as the very weak randomness where the soliton dynamics may approach the one in the limit of zero randomness as in [14]).

Assuming the random potential is a perturbation, the approximate equations for the various parameters in this potential can be derived following the work of Cai et.al. [7]. The resulting

equations derived in Appendix A are

$$\dot{\mu} = 0 , \tag{17a}$$

$$\dot{x} = \frac{2 \sinh(\mu)}{\mu} \sin(k) , \tag{17b}$$

$$\dot{k} = \sinh^2(\mu) \sum_{n=-\infty}^{+\infty} \frac{\varepsilon_n \tanh[\mu(n-x)]}{\cosh[\mu(n+1-x)] \cosh[\mu(n-1-x)]} , \tag{17c}$$

$$\begin{aligned} \dot{\alpha} = & 2[\cosh(\mu) \cos(k) + \frac{k}{\mu} \sinh(\mu) \sin(k)] \\ & + \sinh^2(\mu) \sum_{n=-\infty}^{+\infty} \frac{\varepsilon_n(n-x) \tanh[\mu(n-x)]}{\cosh[\mu(n+1-x)] \cosh[\mu(n-1-x)]} \\ & - \sinh(\mu) \cosh(\mu) \sum_{n=-\infty}^{+\infty} \frac{\varepsilon_n}{\cosh[\mu(n+1-x)] \cosh[\mu(n-1-x)]} . \end{aligned} \tag{17d}$$

Eqs. (17) are integrated numerically with the initial conditions (9). The algorithm used is the 4th-order Runge-Kutta with $\Delta t = 0.001$, and the summations are truncated to a finite window around the center of mass of the soliton. The values of the parameters μ , k , x , and α are inserted in (2). We refer to this solution as the semianalytical solution. We compare this solution with the numerical integration of Eq. (8) (referred as the numerical solution), and the results are presented in Fig. 1. In Fig. 1(a) we compare the center of mass coordinate x of (2) and (11) found in the semianalytical calculation with the numerical solution, and small acceleration is presented for this type of soliton [see also Fig. 1(f)]. It is found that on the average the velocity of the semianalytical solution is somewhat larger than the one found numerically. In Fig. 1(b) the velocity of the center of mass and the second moment are presented. The plots for the velocity are zoomed in Figs. 1(c)-(e). We note that for $t < 100$ there is excellent agreement between the numerical and the semianalytical results. At the time $t > 100$ the second moment increases rapidly, therefore the approximation (17) is not justified anymore, and large deviation between the two solutions are shown. In Fig. 1(f), the semianalytical velocity for longer time and its linear fit are presented.

B. The regime $\mu \approx 1$

As a representative example in this regime, we study a soliton with $\mu = 1$, moving in one realization of the random potential with $W = 0.1$. We solve numerically Eq. (8) with the initial condition (9). In this case the initial width of the soliton is 7 sites ($N_w = 7$). The results are presented in Fig. 2. We find that the center of mass x moves monotonically to the right till a time $t = T_c$ when oscillations start [see Fig. 2(a)]. From Fig. 2(b) we see that the velocity decreases monotonically for $t < T_c$ and oscillates for $t > T_c$. The period of these oscillations decreases with time. From Fig. 2(c) we see that the mass decreases with time and in the first stage this decrease is rapid, therefore the approximation (17) fails. Finally the mass approaches a nonvanishing constant. The interesting phenomenon we find is the trapping of the soliton for

$t > T_c$ as a result of randomness. The particle aspect of this dynamics will be discussed in the next section.

C. The regime $\mu \ll 1$

In this regime, the soliton has a larger width, and it is easier to lose its mass through radiation. With a limit of zero randomness, Garnier [14] shows that the soliton propagates with its mass decreasing to zero, and its velocity to a nonvanishing constant. In fact, the radiation induces a remarkable deformation on the soliton profile after some time of propagation if the randomness is not weak enough. In Fig. 3 we present an example with $\mu = 0.5$ [where the initial width of the soliton is 11 sites ($N_w = 11$)] and $W = 0.1$. The initial condition is (9). From Fig. 3(a) we see that the soliton spreads, and radiates its mass over 300 sites in the time $t = 1000$. From Figs. 3(b) and (c) we conclude that the mass and velocity decrease. Such decrease of velocity contains some short time intervals where the velocity oscillates approximately near a constant. The similar time intervals have been observed in the work of Franzosi et.al. [15], as they studied the mobile discrete breathers propagating on very weak backgrounds in the framework of discrete NLSE. Their time intervals appear to be much longer, with weaker velocity oscillation, since their background perturbation is very weak (of the level $10^{-4} \sim 10^{-3}$). However, we have not observed the trapping behavior in this regime, especially before the soliton undergoes a large deformation.

III. PARTICLE APPROACH FOR SOLITON TRAPPING IN DISORDERED AL LATTICE

In this section we will study the question: Can an AL soliton in a weak random potential be considered as particle?

We will focus on the soliton trapping in the second regime where $\mu \approx 1$, and try to give a particle description of the trapping behavior. We start from the momentum (5), and assume it still to be the momentum for the model (8) when the random potential is weak. Taking a derivative on both sides of Eq. (5) with respect to t , and substituting Eq. (8) into the result, we can obtain

$$\frac{dP}{dt} = 2 \sum_{n=-\infty}^{+\infty} \text{Re}(\psi_n \psi_{n+1}^*) (\varepsilon_n - \varepsilon_{n+1}), \quad (18)$$

where Re means the real part. For derivation see Appendix B. With the assumption that the soliton is particle-like, Eq. (18) can be viewed as the variation rate of its momentum. On the other hand, dP/dt by (7) can be also written as

$$\frac{dP}{dt} = \frac{dM_s}{dt} v + M_s \frac{d^2 x}{dt^2}. \quad (19)$$

Notice that, due to the mass radiation, the term dM_s/dt in Eq. (19) can not be neglected, especially before soliton trapping. Therefore, we can write the randomness-generated *force* in

two ways, one is directly

$$F_1 = M_s \frac{d^2x}{dt^2} , \quad (20)$$

using (18) and (19) we derive

$$F_2 = 2 \sum_{n=-\infty}^{+\infty} \text{Re}(\psi_n \psi_{n+1}^*) (\varepsilon_n - \varepsilon_{n+1}) - \frac{dM_s}{dt} v . \quad (21)$$

The test of the particle-like picture is performed by comparing the forces F_1 and F_2 presented in Fig. 4. Excellent agreement is found. These results strongly support the description of solitons as particles. In this picture with the force F_2 we associate work done on the soliton that decreases its kinetic energy with an effective potential

$$U(t) = U_0 - \int_{t_0}^t F_2 v dt' , \quad (22)$$

where U_0 is an parameter which can be viewed as the initial energy to be determined as the constant that leads the mean of U , over the time interval of trapping in simulations, to be zero, i.e., $U_0 = \langle \int_{t>T_c} F_2 v dt \rangle$. With the same data, we plot both of this effective potential $U(t)$ and soliton velocity in Fig. 4(e). It shows that the first reflection ($T_c \approx 1100$), with the soliton velocity changing its sign, occurs at a peak position of the effective potential. Also other changes in the direction of motion of the soliton take place at maxima of $U(t)$ as can be seen from Fig. 4(e). This is a direct result of (22) since

$$\frac{dU(t)}{dt} = -F_2 v , \quad (23)$$

therefore $\frac{dU(t)}{dt} = 0$ implies either $F_2 = 0$ or $v = 0$.

IV. SCALING OF THE TRAPPING TIME T_c

In this section we demonstrate that there exists a scaling relation between the time T_c when the trapping starts and the random potential strength W . In Figs. 5(a) and (b) T_c is plotted as a function of W . It is found that

$$T_c \sim W^{-\eta} , \quad (24)$$

with $\eta = 2.32 \pm 0.41$. For each $W \in [0.06, 0.1]$, we average the function $U(t)$ of (22) over 6 different realizations to derive $U_{ave}(t)$, and plot it till the minimum value of T_c of 6 realizations in Fig. 5(c). From Fig. 5(d), we see that U_{ave} is related to W and t via the combination tW^2 . This suggests the scaling relation

$$U_{ave} \approx \Gamma(tW^2) , \quad (25)$$

where Γ is the scaling function. If trapping starts at the same value of Γ , one finds

$$T_c \propto W^{-2} . \quad (26)$$

Here we want to give some comments on T_c . In forming (24) of this section, we use one realization of random numbers uniformly distributed in $[-1, 1]$, but multiplied by the strength $W/2$, as the random potential. Since change of T_c is obvious for small variation of W [see Figs. 5(a) and (b)], it can generally reflect the scaling relation. One may arrange multiple realizations of random potential to compute the mean value of T_c , as well as its variance possibly, in the statistic sense.

On the other hand, if the randomness is very weak ($W \lesssim 0.04$), Eq. (26) seems to be no longer valid since the soliton can propagate without reflection for very long time as U_{ave} approaches constant (long-time simulation reveals such feature). In this regime, before trapping, the soliton with its mass as almost a constant, loses its velocity very slowly during the very long time propagation in the random potential. In particular, T_c can reach to about 10^5 for $W = 0.02$, and much longer for weaker randomness. We consider this behavior of the soliton to be similar as the *moving breather* in the discrete NLS lattice [15, 16] under very weak noise.

IV. SUMMARY AND CONCLUSIONS

Dynamics of solitons in random potentials was studied in the framework of the Ablowitz-Ladik model [2]. In particular we explored the question when can a soliton be considered as a particle and what are the conditions for trapping of solitons in a random potential. The behavior was classified into three regimes specified by Eq. (16). In the regime $\mu \gg 1$ for short times the approximation (17) holds. In particular μ changes some time resulting in the change of the soliton width. This destroys the semianalytic solution resulting of (17) as is clear from Fig. 1. An improved approach will be subject of future studies. For $\mu \ll 1$ the soliton spreads very quickly and the potential picture is not appropriate.

The most interesting regime is when $\mu \approx 1$. The most interesting phenomenon is that the soliton is trapped and moves as a particle with varying mass. The equality of $F_1 = F_2$ that is demonstrated in Fig. 4 is a strong evidence for the particle nature. The velocity changes its direction at some maxima of the potential (22) as can be seen from Fig. 4(e) and as expected from (23). Better understanding of the potential $U(t)$ and its relation to the average of the random potential over the profile of the soliton will be left for future studies. Finally we found that T_c , the first time when the velocity changes direction, scales with the strength of the random potential according to (25) and the potential is scaling function of time and the strength of random potential (24). This may signal the existence of an underlying statistical theory that should be explored in the future.

ACKNOWLEDGEMENT

Z.-Y. S. acknowledges the support in part at the Technion by a fellowship of the Israel Council for Higher Education. This work was partly supported by the Israel Science Foundation (ISF-1028), by the US-Israel Binational Science Foundation (BSF-2010132), by the USA National Science Foundation (NSF DMS 1201394) and by the Shlomo Kaplansky academic chair.

Appendix A

Refs. [7] show that for an AL model with a perturbation term

$$i\frac{\partial\psi_n}{\partial t} = -(\psi_{n-1} + \psi_{n+1})(1 + |\psi_n|^2) + R_n, \quad (\text{A.1})$$

the soliton parameters in (2) in the adiabatic approximation satisfy the following evolution equations

$$\dot{\mu} = \sinh(\mu) \sum_{n=-\infty}^{+\infty} \frac{\cosh[\mu(n-x)]\text{Im}(r_n)}{\cosh[\mu(n+1-x)]\cosh[\mu(n-1-x)]}, \quad (\text{A.2a})$$

$$\dot{x} = \frac{2\sinh(\mu)}{\mu} \sin(k) + \frac{\sinh(\mu)}{\mu} \sum_{n=-\infty}^{+\infty} \frac{(n-x)\cosh[\mu(n-x)]\text{Im}(r_n)}{\cosh[\mu(n+1-x)]\cosh[\mu(n-1-x)]}, \quad (\text{A.2b})$$

$$\dot{k} = \sinh(\mu) \sum_{n=-\infty}^{+\infty} \frac{\sinh[\mu(n-x)]\text{Re}(r_n)}{\cosh[\mu(n+1-x)]\cosh[\mu(n-1-x)]}, \quad (\text{A.2c})$$

$$\begin{aligned} \dot{\alpha} = & 2[\cosh(\mu)\cos(k) + \frac{k}{\mu}\sinh(\mu)\sin(k)] \\ & + \sinh(\mu) \sum_{n=-\infty}^{+\infty} \frac{(n-x)\sinh[\mu(n-x)]\text{Re}(r_n)}{\cosh[\mu(n+1-x)]\cosh[\mu(n-1-x)]} \\ & - \cosh(\mu) \sum_{n=-\infty}^{+\infty} \frac{\cosh[\mu(n-x)]\text{Re}(r_n)}{\cosh[\mu(n+1-x)]\cosh[\mu(n-1-x)]} \\ & + k\frac{\sinh(\mu)}{\mu} \sum_{n=-\infty}^{+\infty} \frac{(n-x)\cosh[\mu(n-x)]\text{Im}(r_n)}{\cosh[\mu(n+1-x)]\cosh[\mu(n-1-x)]}, \end{aligned} \quad (\text{A.2d})$$

where $r_n = R_n \exp[-ik(n-x) - i\alpha]$. For Eq. (8) with the solution form (2) we have

$$r_n = \frac{\varepsilon_n \sinh(\mu)}{\cosh[\mu(n-x)]}. \quad (\text{A.3})$$

Substituting (A.3) into (A.2) we obtain Eqs. (17).

Appendix B

In this appendix, we will show the derivation of Eq. (18). Take a derivative on both sides of Eq. (5) with respect to t , one can obtain

$$\frac{dP}{dt} = i \sum_{n=-\infty}^{+\infty} \left(\frac{\partial\psi_n}{\partial t} \psi_{n+1}^* + \psi_n \frac{\partial\psi_{n+1}^*}{\partial t} - \frac{\partial\psi_n^*}{\partial t} \psi_{n+1} - \psi_n^* \frac{\partial\psi_{n+1}}{\partial t} \right). \quad (\text{B.1})$$

With Eq. (8), we derive the following sets

$$\frac{\partial \psi_n}{\partial t} = i[(\psi_{n-1} + \psi_{n+1})(1 + \psi_n \psi_n^*) - \varepsilon_n \psi_n] , \quad (\text{B.2a})$$

$$\frac{\partial \psi_n^*}{\partial t} = -i[(\psi_{n-1}^* + \psi_{n+1}^*)(1 + \psi_n \psi_n^*) - \varepsilon_n \psi_n^*] , \quad (\text{B.2b})$$

$$\frac{\partial \psi_{n+1}}{\partial t} = i[(\psi_n + \psi_{n+2})(1 + \psi_{n+1} \psi_{n+1}^*) - \varepsilon_{n+1} \psi_{n+1}] , \quad (\text{B.2c})$$

$$\frac{\partial \psi_{n+1}^*}{\partial t} = -i[(\psi_n^* + \psi_{n+2}^*)(1 + \psi_{n+1} \psi_{n+1}^*) - \varepsilon_{n+1} \psi_{n+1}^*] . \quad (\text{B.2d})$$

Substituting (B.2) into (B.1), after simplification, we can obtain

$$\begin{aligned} \frac{dP}{dt} &= \sum_{n=-\infty}^{+\infty} [\varepsilon_n (\psi_n \psi_{n+1}^* + \psi_n^* \psi_{n+1}) - \varepsilon_{n+1} (\psi_n \psi_{n+1}^* + \psi_n^* \psi_{n+1})] \\ &= 2 \sum_{n=-\infty}^{+\infty} \text{Re}(\psi_n \psi_{n+1}^*) (\varepsilon_n - \varepsilon_{n+1}) . \end{aligned}$$

Thus Eq. (18) is derived.

References

- [1] C. Sulem and P.L. Sulem, *The Nonlinear Schrödinger Equation: Self-Focusing and Wave Collapse*, Springer-Verlag (NY) (1999).
- [2] M. J. Ablowitz and J. F. Ladik, *J. Math. Phys.* **16**, 598 (1975); **17**, 1011 (1976).
- [3] J. C. Bronski, *J. Stat. Phys.* **92**, 995 (1998).
- [4] E. Akkermans, S. Ghosh, and Z. H. Musslimani, *J. Phys. B* **41**, 045302 (2008).
- [5] Y. V. Kartashov and V. A. Vysloukh, *Phys. Rev. E* **72**, 026606 (2005).
- [6] K. Sacha, C. A. Müller, D. Delande, and J. Zakrzewski, *Phys. Rev. Lett.* **103**, 210402 (2009).
- [7] D. Cai, A. R. Bishop, and N. Grønbech-Jensen, *Phys. Rev. E* **53**, 4131 (1996).
- [8] P. G. Kevrekidis, *The Discrete Nonlinear Schrödinger Equation*, Springer-Verlag (Berlin Heidelberg) (2009).
- [9] P. G. Kevrekidis, A. Khare, A. Saxena, I. Bena, and A. R. Bishop, *Math. Comput. Simulat.* **74**, 405 (2007).
- [10] F. G. Bass, Yu. S. Kivshar, V. V. Konotop, and Yu. A. Sinitsyn, *Phys. Rep.* **157**, 63 (1988).
- [11] S. A. Gredeskul and Yu. S. Kivshar, *Phys. Rep.* **216**, 1 (1992).
- [12] J. C. Bronski, *J. Nonlin. Sci.* **8**, 161 (1998).
- [13] J. Garnier, *SIAM J. Appl. Math.* **58**, 1969 (1998).
- [14] J. Garnier, *Phys. Rev. E* **63**, 026608 (2001).
- [15] R. Franzosi, R. Livi, G.L. Oppo, and A. Politi, *Nonlinearity* **24**, R89 (2011).
- [16] T. Neff, H. Hennig, and R. Fleischmann, arXiv.1309.7939v2 (2013).

Figure captions and figures

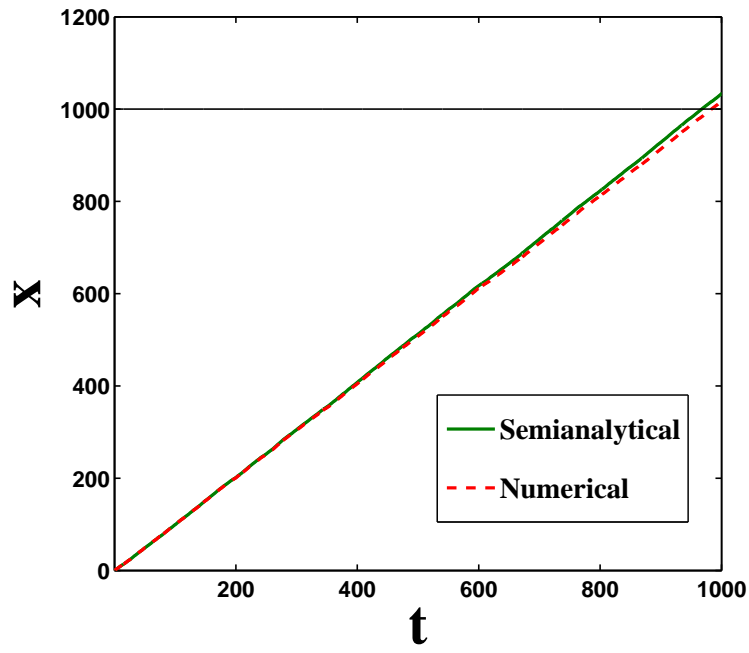


Figure 1(a)

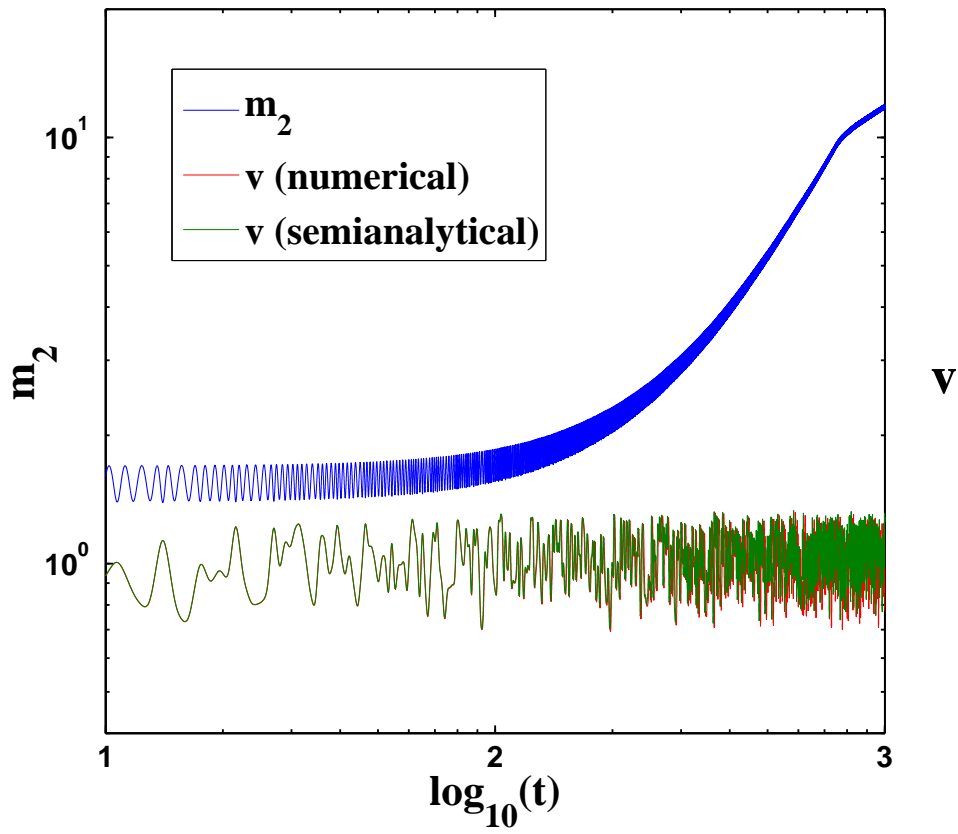


Figure 1(b)

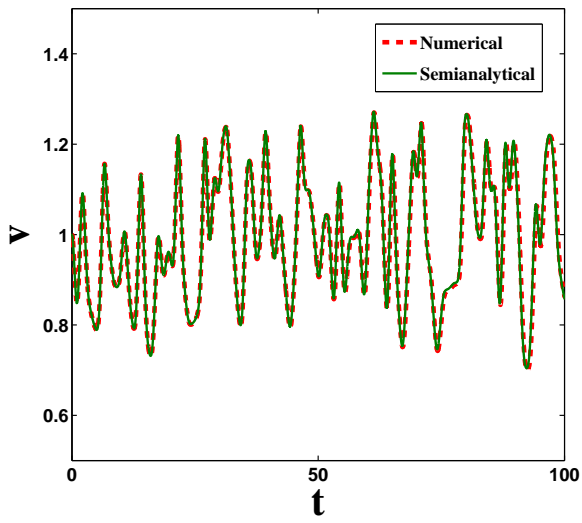


Figure 1(c)

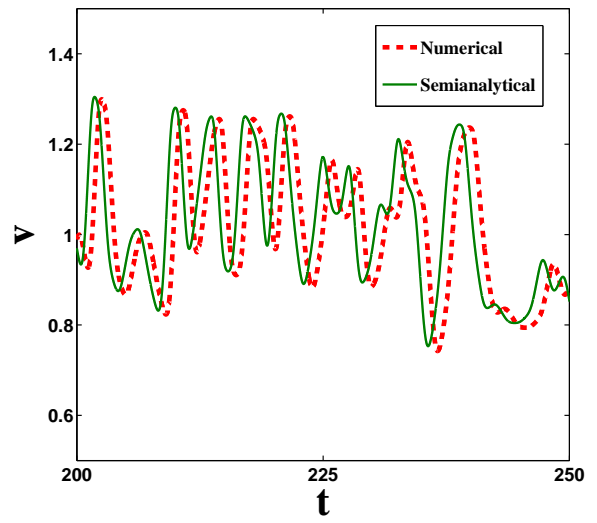


Figure 1(d)

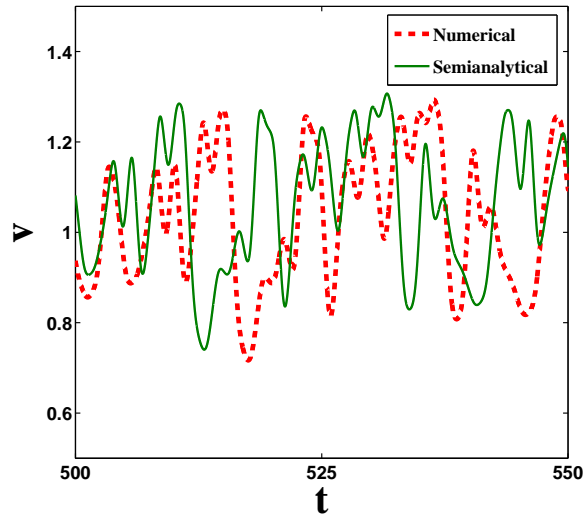


Figure 1(e)

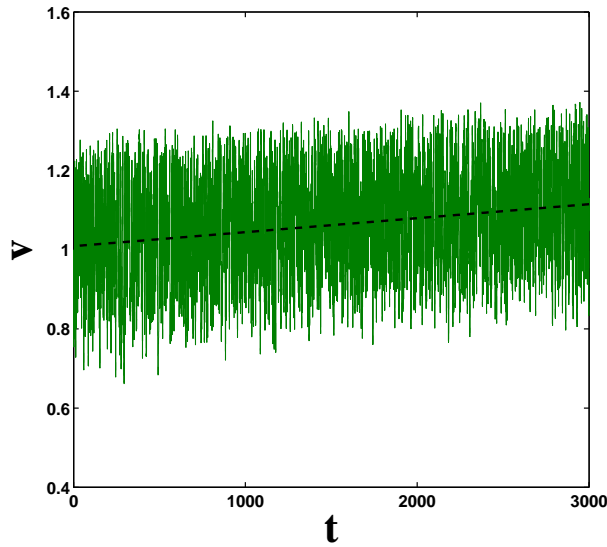


Figure 1(f)

FIGURES 1: AL soliton acceleration by one realization of random potential [$\mu = 3$, $v(t = 0) = 1$, and $W = 0.1$]. (a) Comparison of the center of mass between the semianalytical and numerical results. (b) Comparison of the semianalytical and numerical velocities, and the second moment m_2 . (c)-(e) Zoomed views of the velocity comparison in three different time intervals. (f) Semianalytical velocity by solving Eqs. (17), and the dashed line is the linear fit of the data.

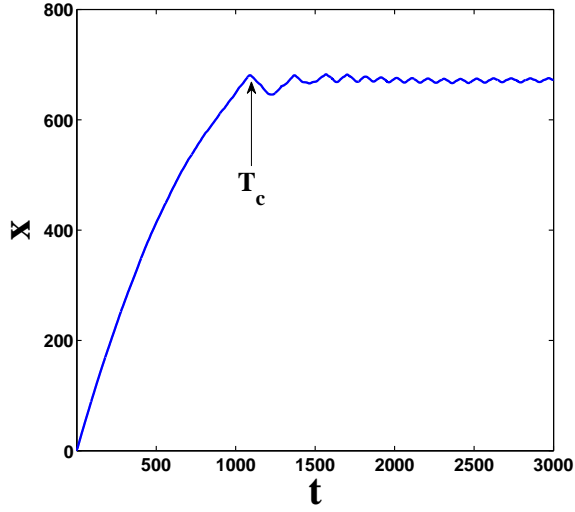


Figure 2(a)

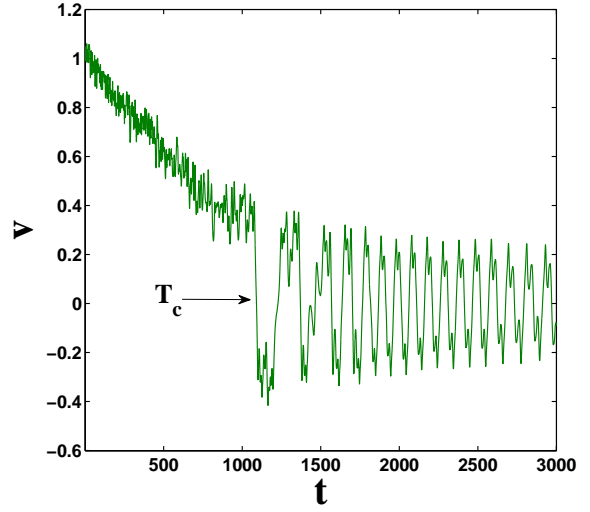


Figure 2(b)

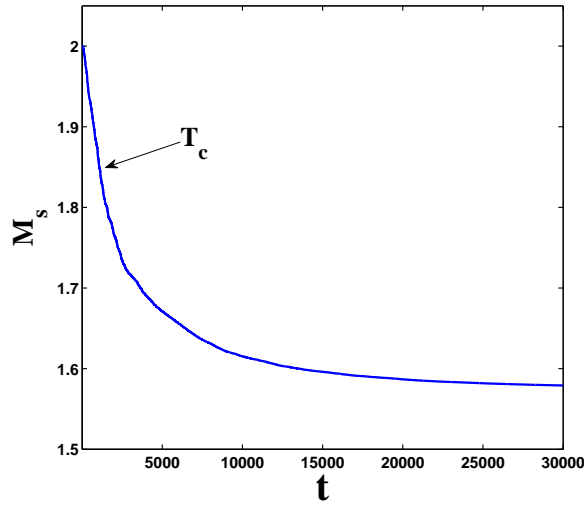


Figure 2(c)

FIGURES 2: AL soliton trapping by one realization of random potential [$\mu = 1$, $v(t = 0) = 1$, and $W = 0.1$]. (a) Center of mass x [Eq. (11)] as function of time t . (b) The soliton velocity v [Eq. (13)] as function of time t . (c) The mass M_s [Eq. (10)] as function of time t .

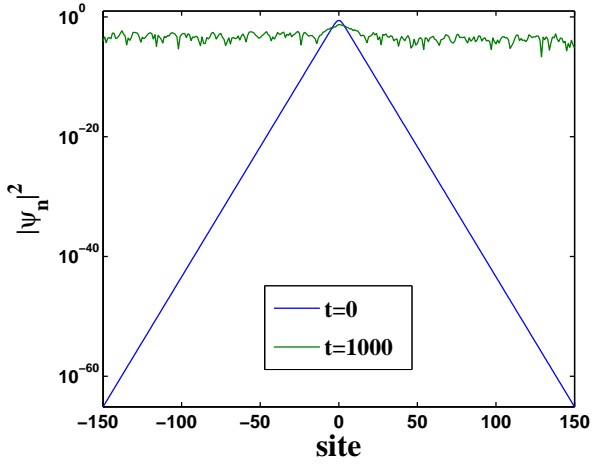


Figure 3(a)

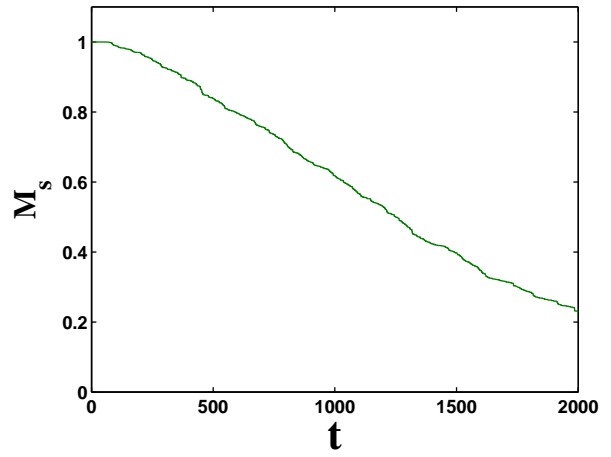


Figure 3(b)

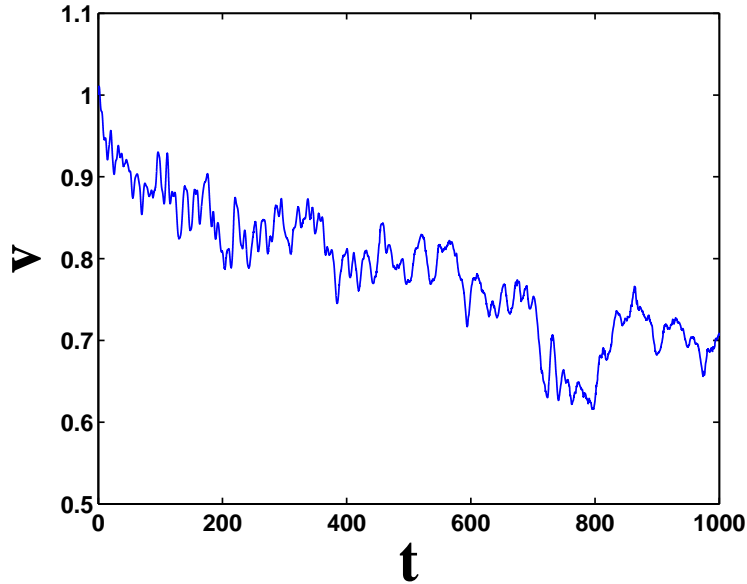


Figure 3(c)

FIGURES 3: AL soliton propagation in one realization of random potential [$\mu = 0.5$, $v(t = 0) = 1$, and $W = 0.1$]. (a) The soliton profiles at $t = 0$ and $t = 1000$ (note that the site coordinate is fixed on the center of mass). (b) The mass M_s [Eq. (10)] as function of time t . (c) The soliton velocity v [Eq. (13)] as function of time t .

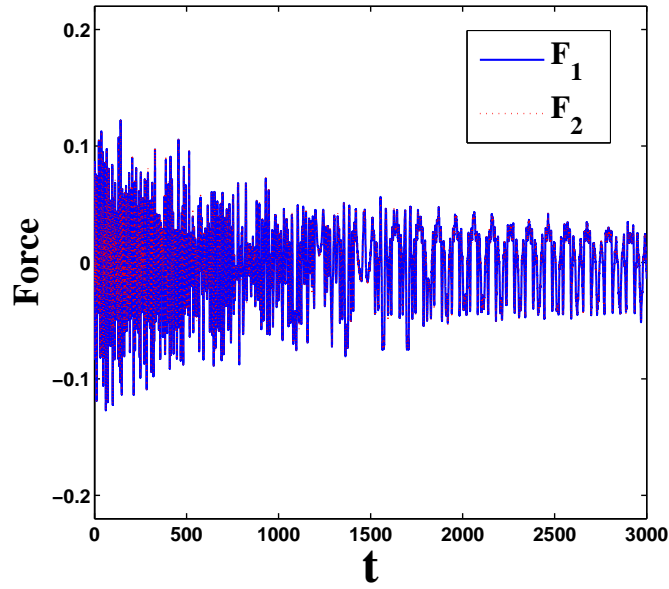


Figure 4(a)

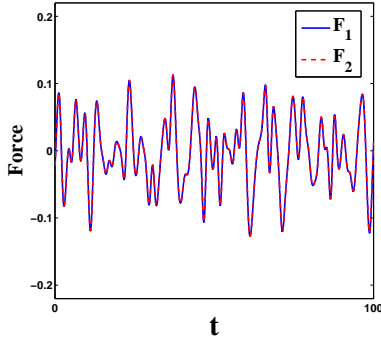


Figure 4(b)

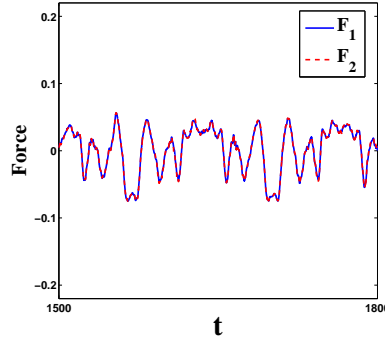


Figure 4(c)

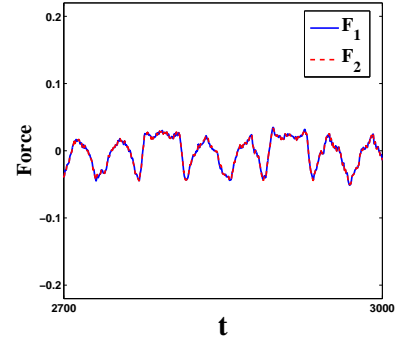


Figure 4(d)

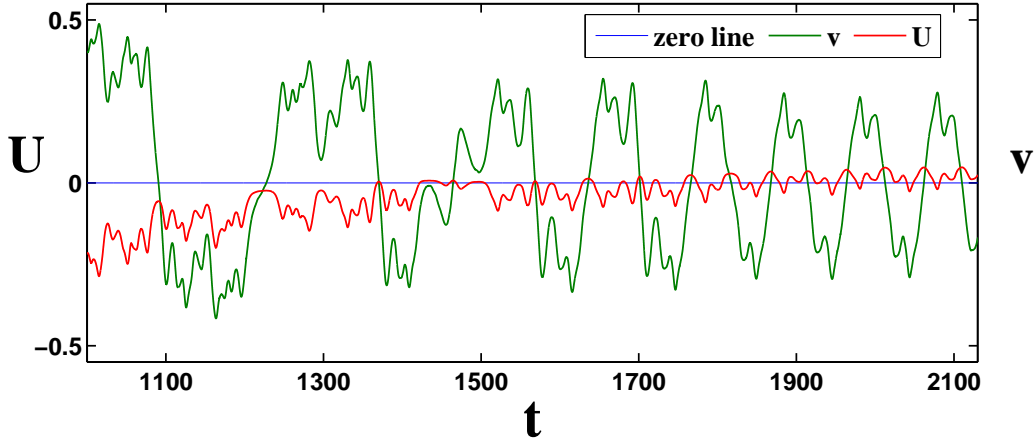


Figure 4(e)

FIGURES 4: (a) Comparison of the two forces F_1 [Eq. (20)] and F_2 [Eq. (21)] with the soliton parameters and random potential the same as those in Figs. 2(a) and (b). (b)-(d) Zoomed views of the panel (a) for three different time intervals. (e) The effective potential U and soliton velocity v after the soliton's first reflection ($T_c \approx 1100$).

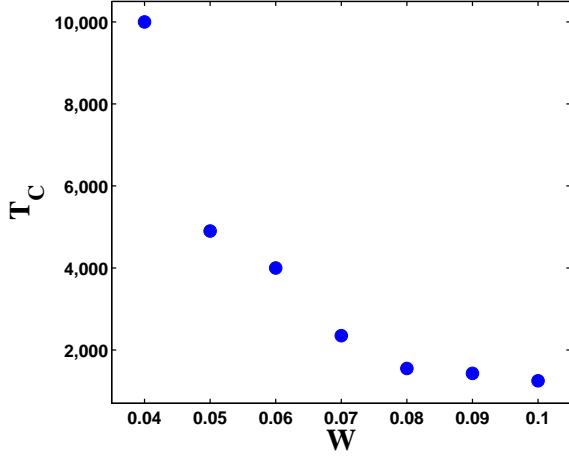


Figure 5(a)

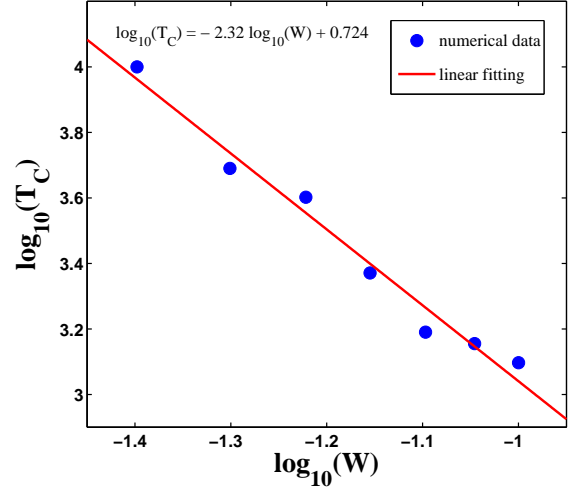


Figure 5(b)

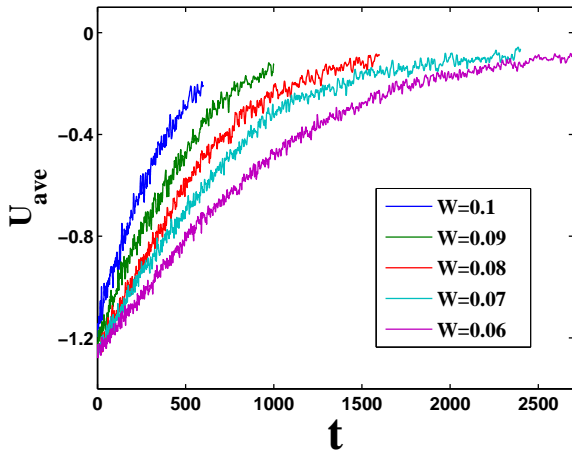


Figure 5(c)

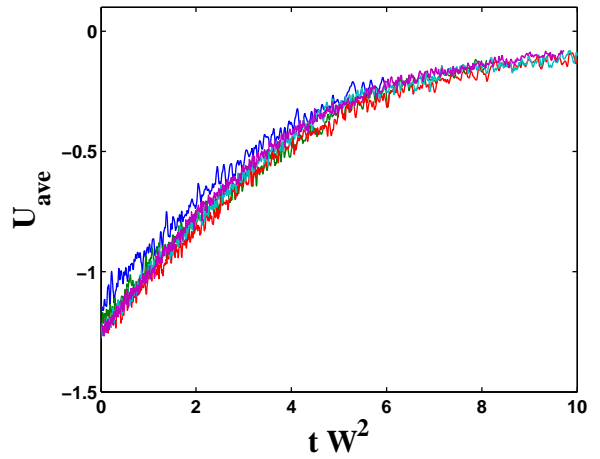


Figure 5(d)

FIGURES 5: (a) T_c as function of W . The random potential are consisted of one realization of random numbers in $[-1, 1]$, multiplied by different strength $W/2$. (b) Linear fit of the data (logarithm forms of variables) in (a). (c) U_{ave} as function of t and W . (d) U_{ave} as a function of the scaling variable tW^2 .